Paleomagnetic and gravimetrical reconnaissance of Cretaceous volcanic rocks from the Western Colombian Andes: Paleogeographic connections with the Caribbean Plate

SANTIAGO HINCAPIÉ-GÓMEZ[1], AGUSTÍN CARDONA[2], GIOVANNY JIMÉNEZ[3], GASPAR MONSALVE[1], LEÓN RAMÍREZ-HOYOS[1] AND GERMÁN BAYONA[4]

1 Departamento de Geociencias y Medio Ambiente, Universidad Nacional de Colombia, Medellín, Colombia (sahincapiego@unal.edu.co)

2 Departamento de Procesos y Energía, Universidad Nacional de Colombia, Medellín, Colombia

3 Departamento de Geología, Universidad Industrial de Santander, Bucaramanga, Colombia

4 Corporación Geológica Ares, Bogotá, Colombia

Received: August 3, 2016; Revised: January 4, 2017; Accepted: June 11, 2017

ABSTRACT

The reconstruction of the tectonic evolution of the oceanic crust, including the recognition of ancient oceanic plumes and the differentiation between multiple and single oceanic arcs, relies on the paleogeographic analysis of accreted oceanic fragments found in orogenic belts. Here we present paleomagnetic and gravity data from Cretaceous oceanic basaltic and gabbroic rocks, the continental metamorphic basement, and their associated cover from northwestern Colombia. Based on regional scale tectonic reconstructions and geochemical constraints, such rocks have been interpreted as remnants of an oceanic large igneous province formed in southern latitudes, which was accreted to the sialic continental margin during the Late Cretaceous. Gravity analyses suggest the existence of a coherent high density segment separated by major suture zones from a lower density material related to the continental crust and/or thick sedimentary sequences trapped during collision. A characteristic paleomagnetic direction in Early and Late Cretaceous oceanic volcano-plutonic rocks, revealing a southeastern declination (D) and a negative inclination (I), may be interpreted in two different ways: (1a primary magnetization (tilt-corrected direction D = 130.3°, I = –23.3°, k = 23.4, α_{95} = 26.4°), suggesting clockwise rotation around 130°, and magnetization acquired in southern latitudes (range of 4°S to 21°S); or (2) a remagnetization event during a reverse interval of the Earth's magnetic field in the Cenozoic (in situ direction D = 128.7°, I = –6.2°, k = 23.1, α_{95} = 26.1°), suggesting a counter-clockwise rotation around 50°. The first scenario seems more plausible, as it is consistent with previous paleomagnetic studies at other localities; it is compatible with a southern paleogeography for this block, and when

integrated with other regional geological and paleomagnetic studies, supports a southern Pacific origin of a major oceanic block, formed as a part of a broader Cretaceous plateau that may have extended south or southwest of Galapagos. After its initial accretion, this block was subsequently fragmented due to the oblique SW-NE approach to the continental margin during the Late Cretaceous.

K e y w o r d s : paleomagnetism, gravimetry, Cretaceous, Western Colombia, Caribbean Plate

1. INTRODUCTION

Continental margins are modified by the accretion of oceanic terranes, which include island arcs, oceanic plateaus, and/or seamounts that commonly travel from an intra-oceanic position to reach the continental margin and cause major orogenic events and compositional modifications to the continental crust (*Cawood et al., 2009*).

Whereas some of these oceanic terranes are an expression of the long term plate tectonic evolution of convergent and divergent plate boundaries (e.g., island arcs, mid-ocean ridge basalt - MORB), other fragments may represent the vestiges of more catastrophic processes that record deep mantle or core-mantle instabilities that end up in the formation of mantle plumes that are emplaced into the surface as major volcanic provinces (*Hoernle et al., 2002*).

To appropriately reconstruct the tectonic evolution of ancient orogens, evaluate plate kinematic interactions, and hypothesize about the existence of non-standard plate tectonic instabilities that modified the oceanic crust, it is necessary to recognize the tectonic setting of the oceanic terranes, their paleogeography, and their history of accretion to the continental margin (*Hoernle et al., 2002*; *Safonova et al., 2009*).

Geophysical data from the Caribbean sea have suggested that its oceanic crust is thicker than normal oceanic crust, reaching values of ca. 18 km (*Case et al., 1990*; *Mauffret and Leroy, 1997*; *Diebold et al., 1999*), whereas geochemical constraints from deep sea recovered samples have indicated that it was formed in association with an enriched mantle source. These two types of observations have been used to suggest that the oceanic crust was formed as part of a large igneous province linked to a mantle plume (*Sinton et al., 1998*).

Similarly, the Cretaceous oceanic volcanic rocks found in the Circum-Caribbean margins, including the Leeward Antilles and the Greater Antilles, and those exposed in the Western Cordillera of the Colombian and Ecuadorian Andes, seem to be related to the Caribbean plate that collided with the margins of the Americas (*Kerr et al., 1997*; *Vallejo et al., 2006*; *Hastie et al., 2008*; *Villagómez et al., 2011*; *Wrigth and Wyld, 2011*; *Spikings et al., 2015*).

Due to the absence of earliest Aptian to earliest Campanian seafloor magnetic anomalies that could be used to constrain plate tectonic reconstructions (*Counil et al., 1989*; *Acton, 2000*), the paleogeography of the Caribbean plate has been the focus of an extensive debate between two contrasting models (Fig. 1; *Pindell and Keenan, 2009*). One model claims for an in-situ origin, in which the oceanic crust formed after the separation of the Americas in the Late Jurassic-Early Cretaceous, and was subsequently covered and

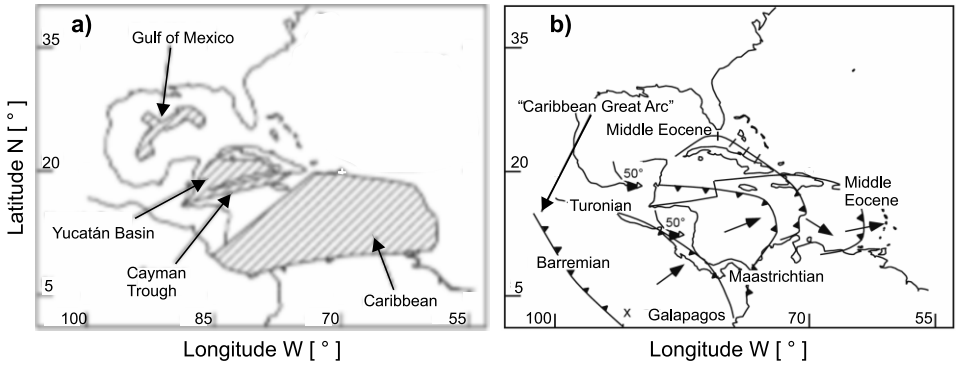

Fig. 1. Two contrasting models for the origin of the Caribbean Plate. **a)** In-situ model (*James, 2006, 2009*); **b)** allocthonous Pacific derived model. Modified after *James (2006)*. © UB-ICTJA.

intruded by an oceanic plateau formed in the same position (Fig. 1a; *James, 2006, 2009*). In contrast, an alternative model considers that the Caribbean plate is allochthonous and was formed in a southwestern position associated with a Pacific plume that migrated to its current location, consuming the former oceanic crust that separated the Americas (Fig. 1b; *Burke, 1988*; *Pindell and Barret, 1990*; *Kerr et al., 1997*).

Based on the integration of geological evidence, including comparisons of the geological record in the continental margins of the Americas and in the accreted oceanic terranes, tomographic interpretations of a subducted Atlantic slab under the Caribbean, and the history of the opening of the Cenozoic Cayman ridge, the allochthonous plate tectonic model for the Caribbean plate has gained great acceptance (reviews in *Pindell and Keenan, 2009*), and it has raised new questions concerning the location of the mantle plume that formed the oceanic plate and its connection with the Galapagos hot spot (*Boschman et al., 2014*).

Gravity surveys in the northwestern Colombian Andes suggest large density contrasts. Positive Bouguer anomaly values (+75 mGal) exist at the western flank of the Western Cordillera (Fig. 2); this anomaly was referred by *Case et al. (1971)* as the "West Colombian high", which decreases abruptly to the east, above the Central Cordillera (Fig. 2). Bouguer anomalies keep decreasing toward the east, not as steeply as above the Western Cordillera, but enough to reach negative values of −100 mGal on top of the mountain range (*Case at al., 1971*; *ANH, 2008*). These gravity contrasts are strongly influenced by geologic units, and could be related with juxtaposed high and low density terranes that include the accreted remnants of the Caribbean plate.

In this contribution, we evaluate gravity data and paleomagnetic results from the northwestern segment of the Western Cordillera of Colombia (Fig. 2), where oceanic plateau related basaltic and gabbroic crust is discontinuously exposed (*Nivia, 1996*; *Kerr et al., 1997*; *Villagómez et al., 2011*; *Rodriguez and Arango, 2013*; *Spikings et al., 2015*). These igneous rocks are covered by major siliciclastic sequences and extensive vegetation.

Our approach is used to: (1) elucidate the regional continuity of the high density basaltic crust that formed western Colombia (*Case et al., 1971*), (2) evaluate the

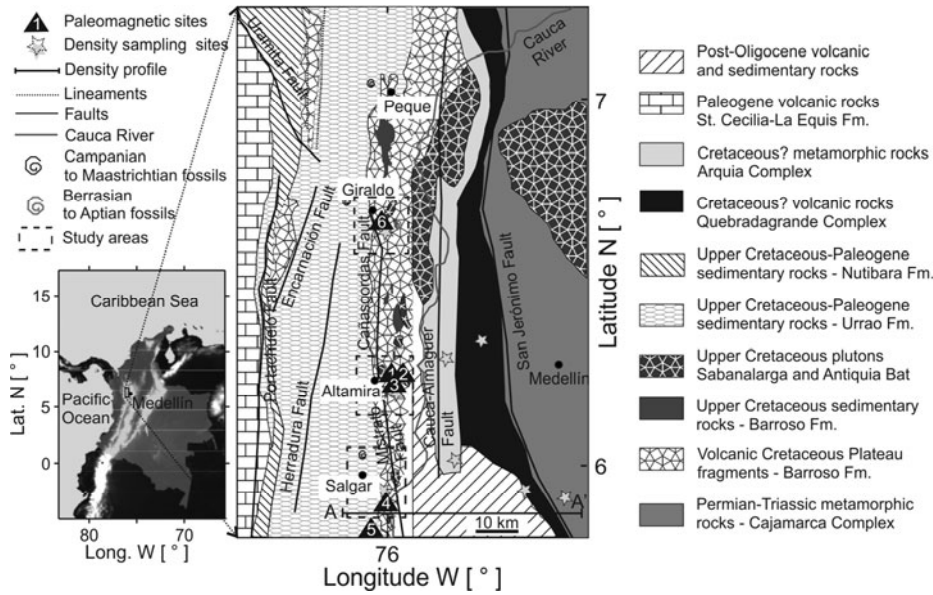

Fig. 2. Geological map from the northern segment of the Western Cordillera and the western flank of the Central Cordillera of Colombia, NW Antioquia State (modified from *Gonzalez, 2001*). A-A' is the gravimetric profile. The numbers inside the triangles represent the paleomagnetic sampling site: 1. B-01, 2. P-02, 3. G-01, 4. P-02, 5. S-01, and 6. P-04.

paleogeography and vertical-axis rotations of the accreted basic oceanic fragments in the Cordillera, and (3) discuss their relations with the Caribbean plate tectonic reconstructions.

Regional gravity can be used to evaluate the plausibility of the idea of juxtaposed terranes. In previous works, gravity anomalies were used to describe the transitions among different terranes, by estimating crustal thicknesses (e.g., *Manalo et al., 2015*), or by delineating tectonic physiographic features such as trenches, paleo trenches, arches, etc. (e.g., *Franco and Abbot, 1999*). In this approach, we use a density structure, constrained by some laboratory measurements, to fit the gravity anomalies and test the idea of different crustal blocks.

Former paleomagnetic constraints in western Ecuador, southern Colombia and Panama have documented widespread block rotations and northern paleolatitudinal displacement of Cretaceous oceanic rocks, which have supported the allochthonous tectonic model (*Roperch et al., 1987*; *MacDonald et al., 1997*; *Luzieux et al., 2006*; *Montes et al., 2012*). In this study, new paleomagnetic results from upper Cretaceous basic volcanic and plutonic rocks of the Barroso Formation associated with oceanic plateau and arc environments in the northern segment of the Western Cordillera of the Colombian Andes (Figs 2b and 3) are used to test block translation and vertical-axis rotation. These results are included in the discussion of the Caribbean paleogeographic model.

2. GEOLOGICAL SETTINGS

The Colombian Andes include an extensive Cretaceous record within the three main Cordilleras that form the Northwestern Andean chain (Fig. 2). Each cordillera has a dominant tectonic terrane (see description below) limited by regional faults that extend towards Ecuador (Fig. 2). Those faults are considered as boundaries of major terranes that were juxtaposed to form a single block that includes the Late Cretaceous and the Paleogene (*Restrepo and Toussaint, 1988*; *Restrepo et al., 2009*).

The Chibcha Terrane comprises the Eastern Cordillera, the Magdalena Valley and the eastern flank of the Central Cordillera. This terrane is characterized by the record of an Early Cretaceous extensional basin that evolved from a continental to a marine platform environment until it reached a state of thermally controlled subsidence and tectonic quiescence in the Late Cretaceous (*Etayo-Serna, 1989*; *Villamil, 1999*; *Sarmiento-Rojas et al., 2006*). Paleomagnetic results on several localities of Jurassic and Cretaceous rocks suggest that the Chibcha terrane formed at southern latitudes as a part of an Early to Middle Jurassic magmatic arc, and achieved its current position near the eastern Colombia Llanos region in the Late Jurassic-Early Cretaceous as a result of oblique subduction (*Bayona et al., 2006*).

The Chibcha Terrane is separated from the Tahamí Terrane, which forms the Central Cordillera, by the Otú-Pericos fault (*Restrepo and Toussaint, 1988*). The Tahamí Terrane consists of Permian-Triassic and older metamorphic basement rocks and includes micaceous schists, gneisses and amphibolites (*Restrepo et al., 2011*). This terrane was also affected by Early Cretaceous extensional tectonics, and in the Late Cretaceous was intruded by an extensive series of arc related plutons (*Nivia et al., 2006*; *Villagómez et al., 2011*; *Spkings et al., 2016*).

The Calima Terrane includes the Western Cordillera (Fig. 2), and it is separated from the Tahamí Terrane by the Romeral fault system (Fig. 2; *Restrepo and Toussaint, 1988*). This terrane is mostly made of basic Cretaceous volcanic rocks intruded by gabbroic and tonalitic plutons of Cretaceous age, which have been assigned to intra-oceanic plateau and arc-related settings (*Kerr et al., 1997*; *Villagómez et al., 2011*). Based on their geochemical characteristics and temporal constraints, these units have been correlated with rocks from Western Ecuador and the Circum-Caribbean realm, and they have been considered to be part of a single Caribbean Large Igneous Province (CLIP). This province was interpreted as originated in a mantle plume at southern latitudes (*Kerr et al., 1997*; *Luzieux et al., 2006*), and reached its inter-American position during the Late Cretaceous and the Cenozoic (*Vallejo et al., 2006*; *Van der Lelij et al., 2010*; *Wright and Wyld, 2011*; *Villagómez et al., 2011*; *Montes et al., 2012*; *Weber et al., 2015*). As the CLIP approached the northwestern margin of South America, the collision began at some time between the Late Cretaceous and the Paleocene, causing the deformation and juxtaposition of the oceanic terranes against the continental margin (*Villamil, 1999*). The selected area for our paleomagnetic study is in this terrane (Figs 2 and 3).

Between the Calima and Tahami terranes (Central and Western Cordillera), and along the Cauca Valley, there are several highly deformed Lower and Upper Cretaceous volcano-sedimentary rocks with minor plutons, middle to high pressure metamorphic rocks, and Triassic granitoids, which are all included in the Quebradagrande and Arquía

Complexes (*Maya and González, 1995*; *Vinasco et al., 2006*; *Cochrane et al., 2014*). These units have been interpreted as allocthonous slivers of the Cauca-Romeral fault system (*Restrepo et al., 2011*), as they are also separated by some of the major faults of this system, and their tectonic history may be associated with the Cretaceous extension and collisional tectonics.

The western segment of the Western Cordillera and the Pacific coastal area form the Cuna Terrane (Fig. 2; *Restrepo and Toussaint, 1988*; *Restrepo et al., 2009*). It is made of Cenozoic volcanic and plutonic arc rocks, a narrow and deep Cenozoic basin (Atrato

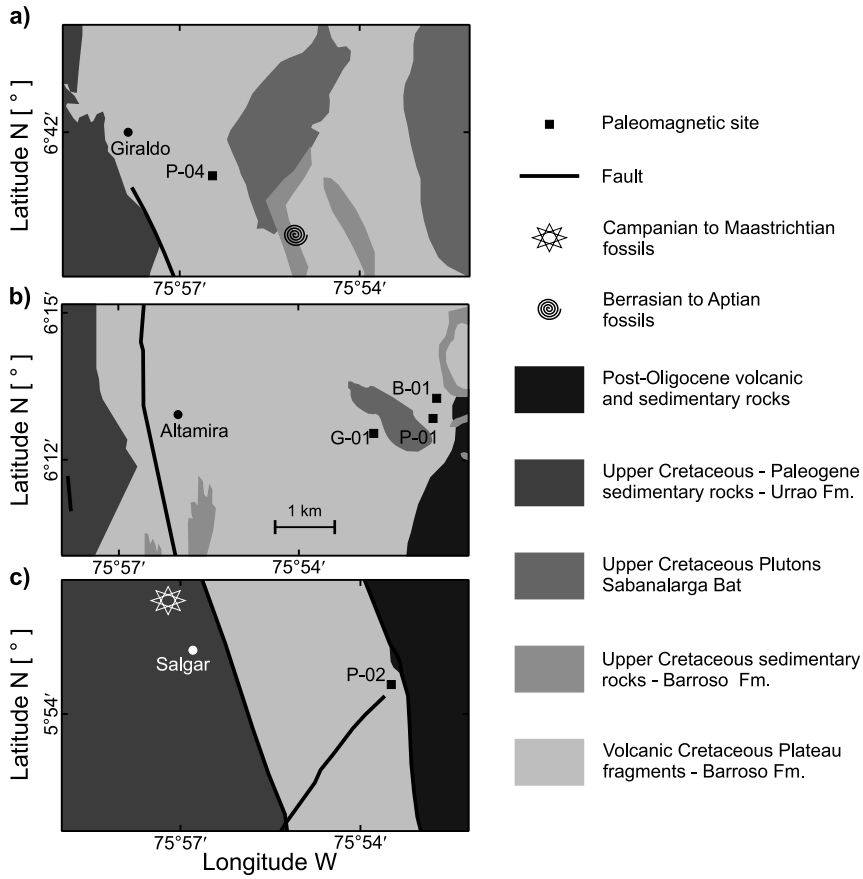

Fig. 3. Geological maps of the paleomagnetic sites: **a)** the Northern region near to Giraldo town. Temporal constraints for the paleomagnetic sites in this region include the 100 Ma Buritica pluton (*Weber et al., 2015*), and Early Cretaceous fossils intercalated with the volcanic rocks of the Barroso Formation (*Gonzalez, 2001*); **b)** the Central region near Altamira town, which is temporally restricted by the intrusion of the Late Cretaceous Altamira Gabbro with ca. 87.6 Ma (*Zapata et al., 2017*); **c)** the Southern region close to Salgar town. Temporal restrictions include the presence of Upper Cretaceous siliciclastic rocks covering the Barroso Formation and associated sediments (*Gonzalez, 2001*).

Basin), and the volcanic rocks from the Serranía de Baudó (*Duque-Caro, 1990*) that include basaltic rocks of oceanic plateau origin, which have yielded Ar-Ar ages between 72 and 77 Ma (*Kerr et al, 1997*). This terrane is considered to be part of the Panama isthmus and was accreted to the continental margin during the Mio-Pliocene (*Duque-Caro, 1990*; *Montes et al., 2015*).

3. REGIONAL GRAVITY

Available gravity data (*Case at al., 1971*; *ANH, 2008*) clearly show major contrasts in the Bouguer anomalies at the northwestern Colombian Andes. Figure 4 illustrates a Bouguer anomaly cross-section in a W-E direction at latitude 5.8°N, and shows that the largest positive anomalies are found over Serranía de Baudó and the western flank of the Western Cordillera in the Calima Terrane (Fig. 2). The gravity profile indicates a positive plateau on top of the Serranía de Baudó, with a drop over the Atrato basin (Figs 2 and 4), where the Bouguer anomaly can reach values as low as −20 mGal; to the east of the basin, the anomaly becomes positive again in the western flank of the Western Cordillera (Fig. 4; *Case et al., 1971*). The transition from the Western to the Central Cordillera is characterized by a further increase in the negative gravity anomaly, reaching values of nearly −60 mGal in the vicinities of the Romeral fault system (RFS, Fig. 4); from this location to the east, gravity anomalies become slightly more negative, but their variations are smoother than those at the western section of the profile (Fig. 4). This gravity structure of the northwestern Andes can be clearly associated to major contrasts in crustal composition and is consistent with the idea of juxtaposed continental and oceanic terranes in the area.

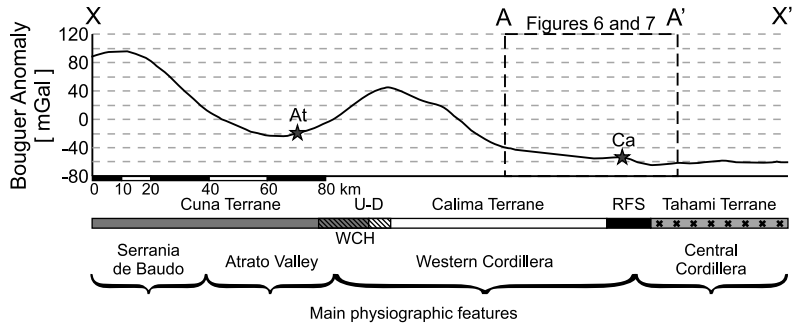

Fig. 4. W-E gravity anomalies regional cross-section at 5.8°N latitude. The thick curve indicates Bouguer anomaly values; dashed square shows the location of A-A' cross-section; see Figs 6 and 7. Lithogenetic terranes and their respective faulted boundaries are mentioned and localized in the middle part of the figure; some physiographic features (bottom) serve as geographic reference in the region. Stars correspond to the location of the At – Atrato and Ca – Cauca rivers. WCH – West Colombian gravity Height, U-D – Uramita-Dabeiba Suture, RFS – Romeral fault system. Location of the cross-section is shown in Fig. 2.

Gravity structure shows roughly an inverse correlation with crustal thickness (*Flueh et al., 1981*; *Yarce et al., 2014*; *Poveda et al., 2015*): the high anomalies of the Western Cordillera are associated with thicknesses of about 30 km, whereas the relatively low anomalies on top of the Central Cordillera correspond to a crustal thickness of nearly 45 km. These contrasts are consistent with the idea of two main domains in the area: an oceanic one, characterized by high values in gravity anomaly, located west of the Romeral fault system, and a continental domain to the east, at the Central Cordillera, which is composed of metamorphic and plutonic rocks of lower density.

4. CRETACEOUS GEOLOGY OF THE WESTERN CORDILLERA

The Western Cordillera of the Colombian Andes is made of a series of Cretaceous elongated belts of volcanic rocks interbedded with sedimentary rocks (*González, 2001*; *Nivia, 2001*; Fig. 2). Volcanic rocks are mainly basaltic in composition, including predominantly lava flows and pillow lavas, with minor tuffs (*Alvarez and Gonzalez, 1979*; *Rodriguez and Arango, 2013*). Geochemical constraints have suggested that most of the flows were formed in an oceanic plateau environment (*Kerr et al., 1997*; *Villagómez et al., 2011*; *Rodriguez and Arango, 2013*), with more limited and not yet precisely defined volcanic-arc rocks (*Rodriguez and Arango, 2013*). Several gabbroic and tonalitic bodies intrude the volcanic units, which are also characterized by plateau and volcanic arc signatures, with U-Pb zircon ages between 100 and 87 Ma (*Ordoñez et al., 2003*; *Villagómez et al., 2011*; *Weber et al., 2015*; *Zapata et al., 2017*).

Absolute and relative age constraints for the volcanic activity are limited and controversial. (1) Ar-Ar ages have yielded 150, 100, 84 and 81 Ma (*González, 2010*; *Rodriguez and Arango, 2013*), (2) intrusive relations with ca. 98 Ma granitoids of plateau origin have been identified, (3) the presence of ca. 88–86 Ma oceanic arc related granitoids has also been documented, and (4) fossils found in sedimentary rocks interbedded with the volcanic rocks have yielded Berrasian to Aptian ages (review in *González, 2001*; Figs 2 and 3). Ar-Ar ages have been difficult to interpret since basalts are generally low-K; the ages have relatively high errors because they have probably been compromised by excess and/or partial argon loss, and may have experienced formation of new potassium bearing alteration phases that will become the main argon reservoir (*Villarraga et al., 2015*).

The clastic belts of the Dagua Group and Penderisco Formation include a series of interbedded sandstone and mudstone layers that change laterally to finer-grained lithologies and chemical sedimentary rocks (*Pardo-Trujillo et al., 2002*) with a Turonian to Maastrichtian fossiliferous record (*Etayo et al., 1989*; *González, 2001*). These sequences are interpreted as turbiditic deposits, and the sandy units include abundant quartz, metamorphic lithics, muscovite and volcanic fragments (*Álvarez and González, 1979*). This association of rock fragments in these turbiditic deposits may be considered as the record of deposition after the accretion of volcanic rocks to the continental margin.

5. METHODS

5.1. Bouguer gravity and density analysis

To evaluate regional gravity anomalies, data were digitized from Bouguer total anomalies map for Colombia, scaled at 1:2 500 000, that is available online from the Colombian Agencia Nacional de Hidrocarburo*s* (National Hydrocarbon Agency). A density of 2.67 g cm^{-3} was used to compute the Bouguer Anomaly and the terrain correction (*ANH, 2008*). We generated profiles with some plausible density distributions to calculate predicted Bouguer gravity data, using the software GravMag (*Burger et al., 2006*), so that we can build a density structure that explains a gravity anomaly profile (*Burger et al., 2006*).

With the purpose of obtaining an approximation to the density structure of the crust in the study area, we collected some relatively unweathered rock samples to measure bulk density in the laboratory. For completeness, we included samples from rocks at both sides of the Romeral fault system, which presumably constitutes the suture zone that separates the continental terranes to the east and the accreted oceanic terranes to the west (*Restrepo and Toussaint, 1988*). For density determination, rock samples were washed and dried at a temperature of 120°C during 12 hours; subsequently, we determined their mass. After this step, we covered the samples in wax, to prevent infiltrations when estimating their weight while suspended and immersed in water. Finally, we calculated density for each sample, so that a mean and a variance could be estimated. Table 1 shows the obtained densities.

5.2. Paleomagnetism: sampling and laboratory tests

We sampled volcanic, plutonic and sedimentary rocks at the northern segment of the Western Cordillera, west of Medellín; a total of 71 cores were obtained from 6 sites (Figs 2 and 3). Paleomagnetic cores were collected with a portable gas-powered drill cooled by water and oriented in situ using a corrected magnetic compass. Samples were taken from three major units: 1) Basaltic and pillow lavas of the Barroso Formation composed mainly of pyroxene and plagioclase that were sampled in 4 sites (Fig. 3); these rocks have geochemical characteristics of plateau affinity and some of them have a few vesicles and amygdales, as well as a weak alteration to epidote, chlorite, sericite and prehnite, which may be related to ocean floor metamorphism during emplacement *(Rodriguez and Arango, 2013*; *Villarraga et al., 2015*; *Zapata et al., 2017*; Fig. 5). 2) One site in fine-grained gabbroic rocks of the Altamira gabbro, which have Upper Cretaceous, ca. 87 Ma zircon ages, and are composed mostly of plagioclase and pyroxene (*Zapata et al., 2017*). 3) One site in interbedded mudstones of the Upper Cretaceous Penderisco Formation.

After field sampling, 71 cores were sliced into 2.2-cm long specimens with a diameter of 2.4 cm. Measurements of the natural remnant magnetization (*NRM*) for paleomagnetic analysis were conducted in a SQUID cryogenic magnetometer (2G enterprises), with a sensitivity of about 1×10^{-8} A m^{-1}, and in an automatic double speed magnetometer AGICO-JR-6A, in the Laboratorio de Palemagnetismo at Sao Paulo University (USPmag).

Table 1. Density values of the rock samples evaluated in this study. C.C. - Central Cordillera, W.C. - Western Cordillera.

Code	Lat. N [°]	Long. W [°]	Rock Type	Lithologic Unit	Avg. Density [g cm^{-3}]	St. Dev. [g cm^{-3}]
GLR-048	6.567	75.812	Schist-Mylonite	Arquia Complex	2.734	0.0314
GLR-049	6.580	75.800	Metagabbro	Arquia Complex	2.970	0.0092
GLR-035	5.909	75.888	Pillow basalt	Barroso Formation	2.765	0.0414
GLR-036	5.900	75.897	Basalt	Barroso Formation	2.984	0.0186
GLR-037	5.848	75.916	Sedimentary rock	Barroso Formation	2.628	0.0185
GLR-038	5.848	75.911	Basalt	Barroso Formation	2.838	0.0213
GLR-046	6.214	75.868	Pillow basalt	Barroso Formation	2.967	0.0122
GLR-047	6.332	75.859	Pillow basalt	Barroso Formation	2.933	0.0311
GLR-051	6.684	75.937	Pillow basalt	Barroso Formation	2.891	0.0157
GLR-087	6.449	75.744	Pillow basalt	Barroso Formation	2.827	0.0040
GLR-088	6.275	75.441	Quartz Diorite	C.C. Intrusive	2.747	0.0143
GLR-089	6.302	75.456	Granodiorite	C.C. Intrusive	2.657	0.0146
GLR-090	6.323	75.467	Quartz Diorite	C.C. Intrusive	2.741	0.0139
GLR-085	5.973	75.586	Schist	Cajamarca Complex	2.638	0.0258
GLR-086	6.329	75.690	Gneiss-Quartzite	Cajamarca Complex	2.728	0.0064
GLR-091	6.329	75.479	Gneiss	Cajamarca Complex	2.661	0.0240
GLR-092	6.330	75.485	Quartzbiotite Gneiss	Cajamarca Complex	2.945	0.0164
GLR-045	6.215	75.875	Gabbro	W.C. Intrusive	2.924	0.0165
GLR-039	5.847	75.908	Gabbro	W.C. Intrusive	2.980	0.0359
GLR-033	6.000	75.807	Basalt	Quebradagrande Complex	2.961	0.0245
GLR-050	6.594	75.779	Basalt	Quebradagrande Complex	2.934	0.0074
GLR-052	6.447	75.740	Basalt	Quebradagrande Complex	2.853	0.0293
GLR-053	6.362	75.720	Basalt	Quebradagrande Complex	2.883	0.0266
GLR-055	6.273	75.787	Basalt	Quebradagrande Complex	2.871	0.0299
GLR-056	6.207	75.711	Basalt	Quebradagrande Complex	2.872	0.0143
GLR-057	6.201	75.705	Basalt	Quebradagrande Complex	2.837	0.0094
GLR-080	5.861	75.570	Basalt	Quebradagrande Complex	2.684	0.0074
GLR-081	5.844	75.578	Basalt-Microgabbro	Quebradagrande Complex	2.636	0.0066
GLR-082	5.841	75.581	Sedimentary rock	Quebradagrande Complex	2.670	0.0100
GLR-083	5.804	75.584	Basalt	Quebradagrande Complex	2.633	0.0242
GLR-084	5.717	75.543	Gabbro	Quebradagrande Complex	2.880	0.0332

A total of 85% of the samples were demagnetized with the alternating field (AF) method, with demagnetization up to 100 mT, using a demagnetizer Molspin Ltd. The measurement of the *NRM* was conducted in an automatic double speed magnetometer AGICO-JR-6A; the other 15% of the samples were passed through thermal demagnetization, through 14–16 heating steps from 100 to 690°C, using a TD-48 oven of ASC Scientific. AF and thermal demagnetization data were plotted on orthogonal vector diagrams (*Zijderveld, 1967*), and the magnetization components were isolated by principal component analysis (*Kirschvink, 1980*). The mean direction of each site was calculated

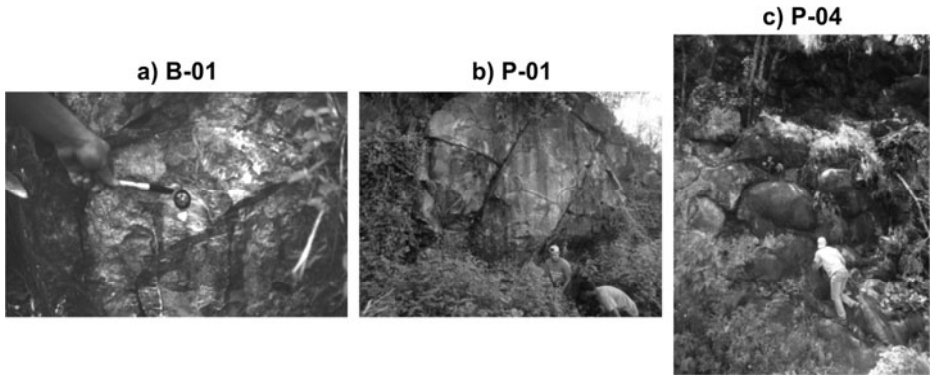

Fig. 5. Some field outcrops of sampled paleomagnetic sites; **a)** basaltic-volcanic rocks (Altamira region), **b)** basaltic and pillow lavas-volcanic rocks (Altamira region), **c)** pillow lavas-volcanic rocks (Giraldo region). See Figs 2 and 3 for the corresponding locations.

using a statistical method on a single sphere (*Fisher, 1953*). The results should be reported as follows: mean direction, a measure of dispersion K, and α_{95} confidence interval.

Thermal demagnetization of three- component isothermal remanent magnetization (*IRM*) (*Lowrie, 1990*) was used to reveal the unblocking temperature of the magnetic minerals. Three different fields were applied to x, y and z axis (0.12, 0.6 and 2.7 T, respectively) in a 755-4K magnetizer (2G Enterprises). A representative core from each site was used for identification of the main magnetic carriers. Low (6 samples) and high temperature (6 samples) thermomagnetic curves were carried out in a CS3 furnace coupled with a KLY-4S Kappabridge (AGICO); because magnetite or other minerals could oxidize due to experimental heating, the process was carried out in an argon atmosphere, later corrected for the susceptibility of the empty furnace.

6. RESULTS

6.1. Density structure and gravity signature of the Western Cordillera

Results of laboratory density analysis yield a density range from 2.63 to 2.98 g cm^{-3}. Rocks from the Barroso Formation, which represent the bulk of the oceanic plateau that has been related to the CLIP, are the ones that yield the highest density, with an average value of ~2.86 g cm^{-3}; rocks to the east of the Romeral Fault Zone, such as those belonging to the Triassic and older metamorphic rocks of the Central Cordillera, and the more recent intrusive bodies (Tahami Terrane), yield average bulk density values of nearly 2.74 and 2.72 g cm^{-3}, respectively (Table 1). The density of those rocks that constitute the basement of the Calima and Tahami terranes decreases from west to east across the study area. Rocks from the Arquia and Quebradagrande Complex, which are closely associated with the Romeral Fault Zone, and might be considered as independent terranes, also show average densities slightly lower than rocks from the Barroso

Formation, with values of ~2.85 and ~2.81 g cm^{-3}, respectively. Even though these densities were measured in samples collected at the surface, they should constitute reasonable estimates for the bulk density of the crust, as our obtained average values are very similar to the mean crustal densities deduced by *Christensen and Mooney (1995)* from seismic velocities.

Taking into account the measured densities, we built a W-E oriented cross-section in which the crust is composed of 1 km wide vertical bars of a single plausible density (Fig. 6, Section A-A' from Figs 2 and 4), whose roots reach Moho depths. We constrained crustal thicknesses using results from *Poveda et al. (2015)* and *Flueh et al. (1981)*, trying to fit the published Bouguer gravity anomalies (*ANH, 2008*). The predicted gravity was calculated using the software GravMag (*Burger et al., 2006*); we forced the densities to be within the interval of those measured in the laboratory, looking for a structure that fits the data reasonably well; at both ends of the profile we also forced the gravity to be the observed one, by assuming masses to the east and west of A-A' with densities and thicknesses similar to those included in the cross-section. For the calculations associated with Fig. 6 we did not put any constraints on specific geological units or lithological boundaries from previous maps; the represented configuration shows a density structure that fits the data with a root mean square (*RMS*) of 0.53 mGal; the high density units are

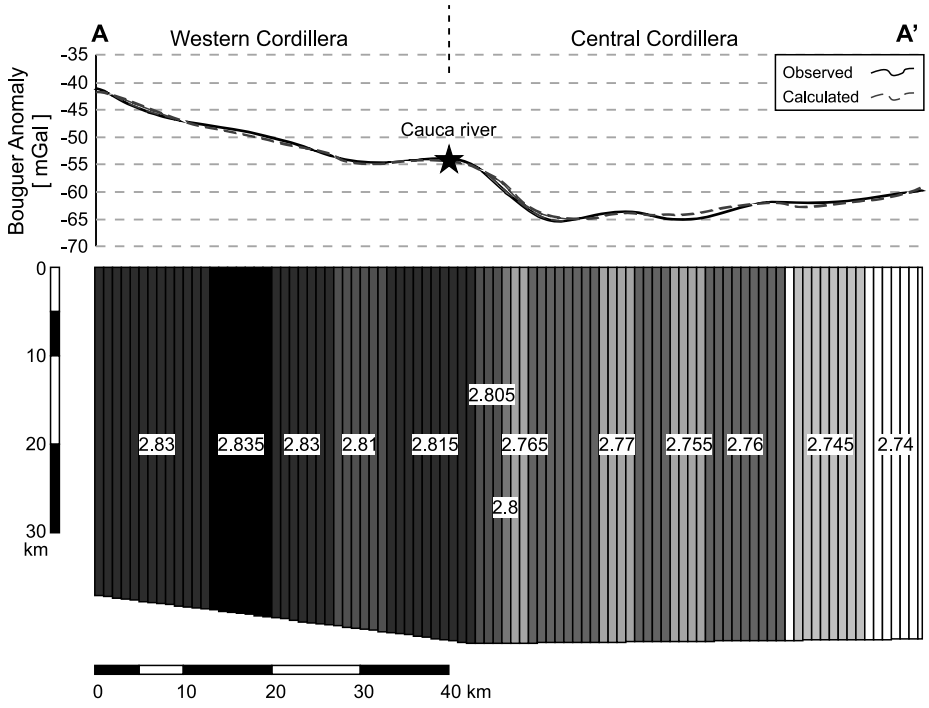

Fig. 6. A-A' profile at 5.8°N. Numbers between columns in the bottom part indicate bulk density values in g cm^{-3} for each block. Root mean square of the difference between the calculated and observed Bouguer anomaly is 0.53 mGal. Location of the A-A' cross-section is shown in Fig. 2.

to the west of the Romeral fault system, and a lower density crust should exist to the east of this feature. We should emphasize the fact that a crustal signal, with very realistic densities and some Moho depth constraints, is enough to fit the airborne Bouguer gravity data. At this latitude, there is no evidence of a high angle West to East subduction, and seismological data supports the idea that in the study area such subduction should be flat (*Chiarabba et al., 2016*; *Syracuse et al., 2016*), so the inhomogeneity that generates the observed gravity anomalies should primarily be in the crust.

Figure 7 takes the same cross-section as in Fig. 6 (Section A-A' from Figs 2 and 4) and fits the gravity using densities similar to those determined in the laboratory, but considering only five units of uniform density that correspond to the main geological units that are thought to constitute the bulk of the crust. The approximate boundaries between units were taken from available geologic maps (*Hall et al., 1972*; *González, 1980*; *González, 2001*). The boundary between the Barroso Formation and the Arquia Complex is covered by a relatively thin sedimentary layer included in the Amaga and Combia formations that may reach 2 km (*González, 2001*), so we infer an approximate limit from

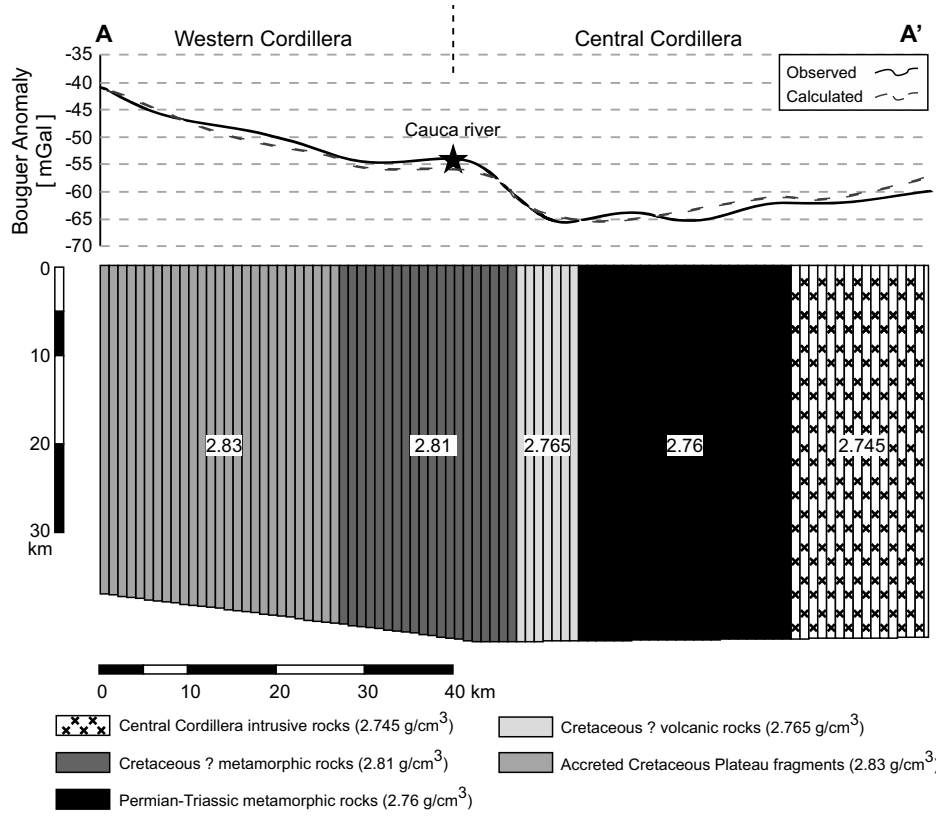

Fig. 7. Geological column-type model for A-A' profile at latitude 5.8°N. Root mean square of the difference between the calculated and observed Bouguer anomaly is 1.29 mGal. Location of the A-A' cross-section is shown in Fig. 2.

a nearby latitude. It is noteworthy that the gravity anomaly can be fitted well (*RMS* of 1.29 mGal) with such a simple crustal structure, so the idea of juxtaposed terranes of different nature in the northwestern Andes results a plausible hypothesis according to the gravity signature.

6.2. Paleomagnetic results

Magnetic mineralogy

The *IRM* thermal demagnetization (*Lowrie, 1990*) gave variable results in the samples analyzed from the six sites (Fig. 8). The soft fraction of the gabbro and basaltic rocks reveals an unblocking temperature of 580°C, indicative of magnetite (Fig. 8a–e). The hard and medium fractions of the basaltic rocks from sites B-01, P-01, P-02, and P-04 are characterized by distinct unblocking temperatures, one about 350–400°C, which is characteristic of maghemite or titanomagnetite, and the second one at 580°C, which suggests magnetite. The soft fraction in the mudstones of site S-01 shows an initial unblocking temperature of 400°C, that suggests the presence of maghemite, and a second unblocking temperature of 570°C that can be associated to magnetite (Fig. 8f); the hard and medium fractions in the same site show an unblocking temperature of 250°C, suggestive of the range of titanomagnetite between 150 and 350°C and a second temperature below 580°C, corresponding to magnetite (Fig. 8f).

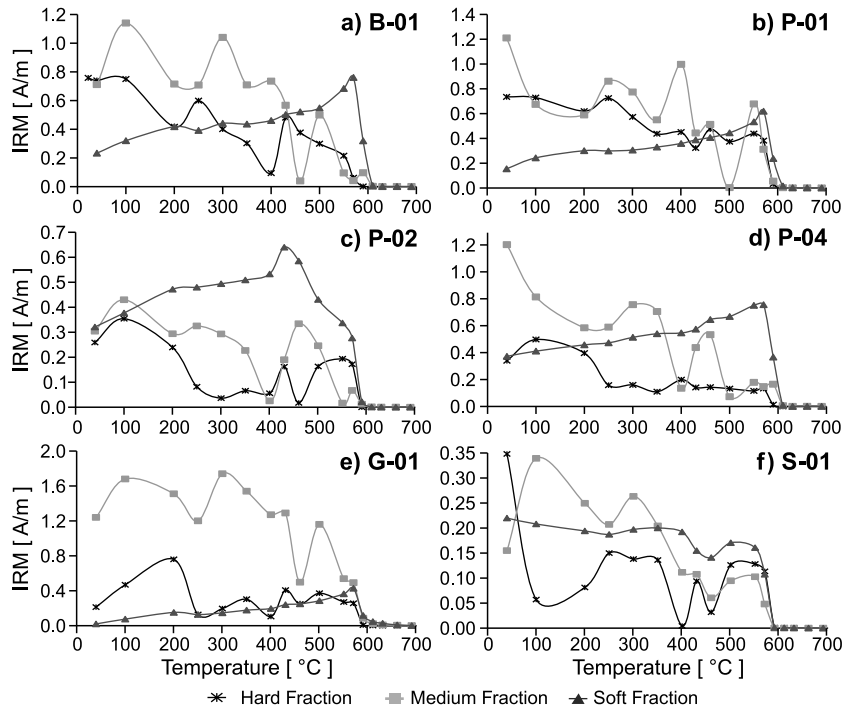

Fig. 8. Thermal demagnetization of the three-component *IRM* according to the method of *Lowrie (1990)* for the specimens of each site: **a)–d)** volcanic rocks, **e)** gabbroic rock, **f)** mudstone.

Low-temperature susceptibility analyses in most of the sites show a dominant ferromagnetic behavior, mainly magnetite as indicated by a well-defined Verwey transition at around 120 K (Fig. 9). Sites B-01, P-04, and G-01 also show a weak paramagnetic contribution (Fig. 9a,c,d). Site P-02 does not show the Verwey transition (Fig. 9b). Thermomagnetic curves during heating up to 700°C were measured to complete the magnetic mineralogy identification. The processes were conducted in a free oxygen environment; new phases were formed at high temperatures (G-01 and P-02). The heating curves show the main decay at around 600°C, confirming magnetite as the dominant magnetic mineral (B-01 and P-04). In general cooling curves show irreversible curves due to mineral changes produced by experimental heating.

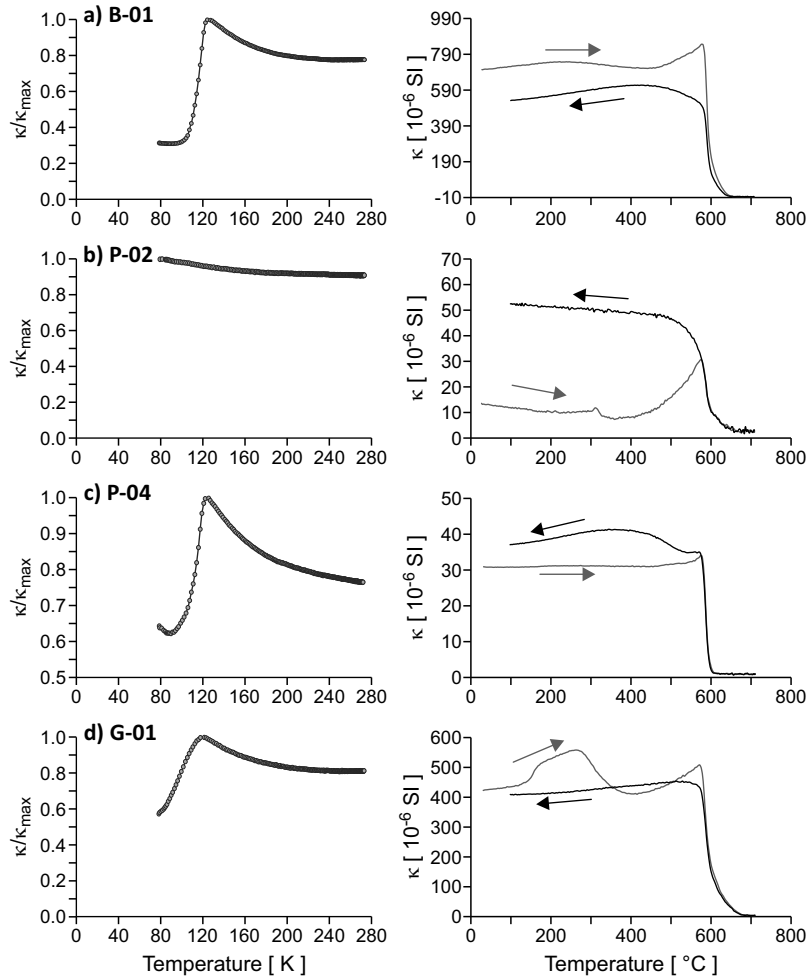

Fig. 9. Temperature dependence of normalized (left) and absolute (right) values of magnetic susceptibility (κ) of four representative samples: **a)–c)** volcanic rocks, **d)** gabbroic rock.

Paleomagnetic directions

The sedimentary site S-01 is characterized by a chaotic behavior during the demagnetizing steps, and therefore it is not possible to uncover a reliable paleomagnetic direction. Paleomagnetic directions at the other five sites show two components (Fig. 10). A weak paleomagnetic component between 0 to 10 mT (site G-01 in Fig. 10) was considered a viscous magnetization and therefore was not used for analysis. The characteristic magnetization component (*ChRM*) was isolated at 30–70 mT (Fig. 10) showing good within-site consistency as indicated by the 95% confidence interval (*Fisher, 1953*) α_{95} values ranging between 8.3° and 14.3° (Table 2, Figs 10 and 11).

The three sites of the Altamira area (two lavas from the Barroso Formation and one Gabbro from sites P-01, B-01 and G-01, Fig. 3b) yielded southeastern directions (in-situ mean direction $D = 128.7°$, $I = -6.2°$, $k = 23.1$, $\alpha_{95} = 26.3°$, where D means declination, I is inclination, and k is the *Fisher (1953)* precision parameter) that after tilt correction shows negative inclinations (tilt-corrected mean direction $D = 130.3°$, $I = -23.3°$, $k = 23.4$, $\alpha_{95} = 26.1°$). The tilt-correction test of the mean paleomagnetic direction of these three sites is not significant to document the timing of magnetization (Fig. 11). The weak variation in k and α_{95} values after tilt correction together with the limited number of reliable sites, do not allow to discriminate the timing of magnetization in relation with the deformation.

Sites P-02 and P-04, from the Salgar and Giraldo regions, respectively, also show southern directions, but differ significantly from the mean direction estimated in the Altamira area. Since they are single sites from different areas we will not use them for paleolatitudinal or rotation analyses. Furthermore, both sites are located near major fault zones and may be affected by local tectonic disturbance.

Rotation values respect to the stable South America craton were evaluated according to *Demarest (1983)*, using the reference South America paleopoles listed in *Torsvik et al. (2008)* (Table 2). The 90–100 Ma age interval does not record significant rotations for the

Table 2. Paleomagnetic results of Late Cretaceous rocks from Western Cordillera. *N*: number of samples measured for directions, *n*: total samples from the site. Bedding is determined using the dip-direction/dip convention (* overturned strata). *K*: the Fisherian precision parameter, α_{95}: the radius of the cone at the 95% confidence level with respect to the mean direction (*Fisher, 1953*).

Site	Formation	Long. W [°]	Lat. N [°]	Age	*N*	*n*	Bedding	In-Situ		Tilt Corrected		*k*	α_{95} [°]
								D	*I*	*D*	*I*		
B-01	Barroso	75.8614	6.2192	>90	6	11	94/24	139.1	8.8	139.0	–8.3	25.50	13.5
P-01	Barroso	75.8623	6.2150	>90	10	14	160/15	128.9	–10.3	126.5	–23.0	34.65	8.3
P-02	Barroso	75.8869	5.9087	>90	11	13	340/51*	236.9	5.1	254.2	–13.3	13.08	13.1
P-04	Barroso	75.9411	6.6863	>100	9	12	7/11	158.0	23.9	154.9	33.4	13.96	14.3
G-01	Altamira	75.8798	6.2117	89.8	8	11	94/24	117.9	–16.8	123.6	–38.3	24.58	13.8
S-01	Penderisco	75.9406	5.8235	70–80	0	10	235/70						

Pole 100 Ma (*Torsvik et al., 2008*): Longitude 312.7°E, Latitude –85.5°N, $\alpha_{95} = 4.1°$

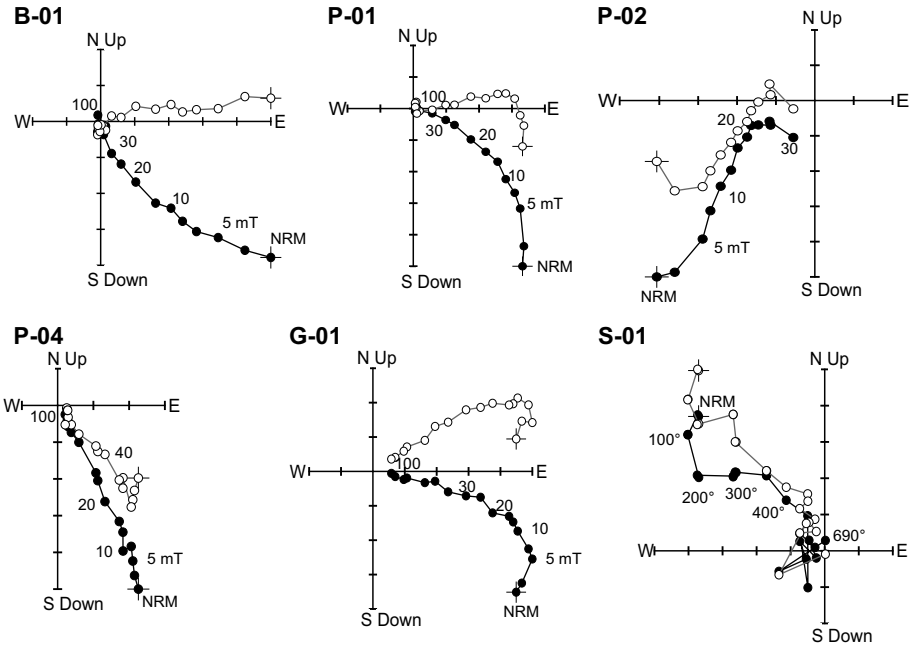

Fig. 10. Orthogonal vector diagrams (*Zijderveld, 1967*) of typical demagnetization data. All directions are plotted in geographic coordinates; full and open dots represent projections on the horizontal and vertical planes, respectively.

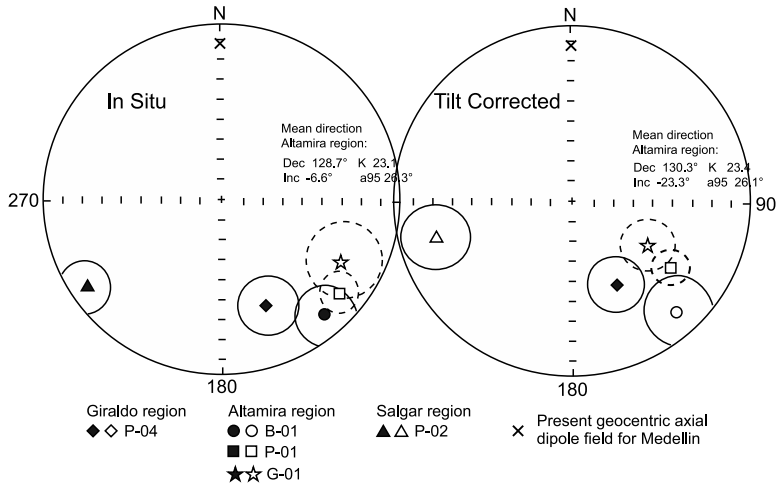

Fig. 11. Equal area projections of the mean site paleomagnetic directions from the study area; solid and open symbols represent positive and negative inclination, respectively. The present normal geocentric axial dipole (GAD) for Medellín latitude (6.2°N) has declination $D = 0°$ and inclination $I = 12.34°$.

stable South America craton (*Torsvik et al., 2012*), and the expected direction in the Altamira area is $D = 358°$ and $I = 4.5°$, which is very similar to the present-day dipole direction: $D = 0.0°$ and $I = 12.3°$ (Fig. 11).

7. DISCUSSION

7.1. Crustal structure

Variations in crustal thickness, with values around 30–35 km beneath the Western Cordillera and greater than 42 km beneath the Central Cordillera (*Flueh et al., 1981*; *Poveda et al., 2015*), together with a gravity signature characterized by a less dense continental block to the east of the Romeral Fault Zone (Tahami Terrane) in the Central Cordillera, and an oceanic, denser, terrane to the west, represented mainly by the Barroso Formation (Calima Terrane) in the Western Cordillera, support the idea of different tectonic terranes with different geological histories.

In Fig. 6 we proposed a density distribution with a Moho depth that fits the airborne gravity anomalies. We did not intend to make an image of the crust, but to evaluate the plausibility of different crustal blocks of distinct nature; the fact that the gravity data is reasonably well reproduced by this density distribution supports the concept of accreted terranes. The transition from the oceanic domain in the west to the continental one in the east occurs across the Arquía and Quebradagrande Complex, which are relatively narrow (less than 40 km wide) and clearly associated with the Romeral Fault Zone.

West of the study area (western locations of cross-section X-X' in Figs 2 and 4), the continuity of the positive gravity values between the Serranía de Baudó and the Western Cordillera is disrupted by a low gravity anomaly over the Atrato Basin, that is related to the presence of a thick sedimentary sequence (*Case et al., 1971*; *Duque-Caro, 1990*), which may be associated with a suture zone (The Uramita Fault, associated to the Dabeiba Suture) that separates the continental margin from the Panama block that was accreted in the Late Neogene (*Duque-Caro, 1990*; *Montes et al., 2015*). This idea was proposed by *Restrepo and Toussaint (1988)* using purely geological arguments, but we speculate that the gravity low is directly related with such a suture.

The continuous character of the gravity high west of the Atrato Basin, where the Barroso Formation is exposed along the axis and the eastern flank of the Western Cordillera, also suggests that this block may represent a coherent tectonic fragment.

7.2. Paleogeographic constraints

Regional scale tectonic and paleogeographic reconstructions for the Northern Andes and the Caribbean realm have suggested that most of the oceanic volcanic rocks that are exposed in the western Andes of Colombia, Ecuador and the Antilles, as well as the Caribbean oceanic plate, were formed as a single oceanic plateau (Fig. 12). Those volcanic rocks grew either in-situ over the oceanic lithosphere formed by the separation of the Americas in the Middle Mesozoic (*James, 2006, 2009*; Fig. 1a), or as a part of the Pacific Plate that migrated from southern latitudes near Galapagos or further west to achieve its current position in the Cenozoic (*Pindell and Keenan, 2009*; Fig. 1b). These models have been reconstructed from the identification of a thick Caribbean oceanic crust,

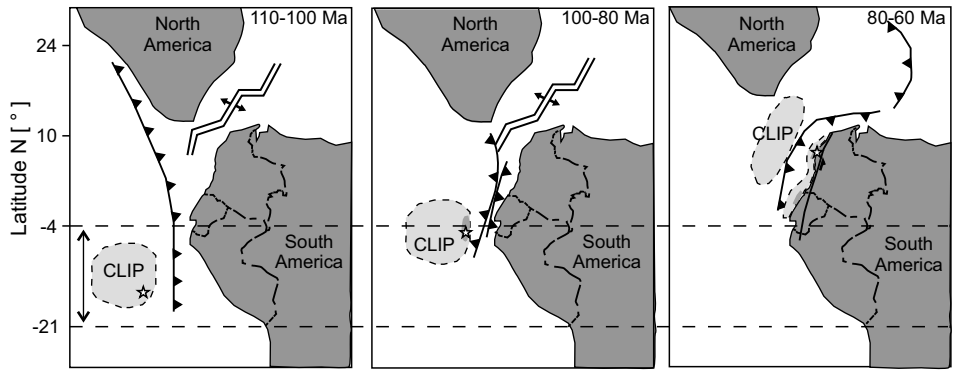

Fig. 12. Cretaceous Paleogeographic model for the Northern Andes and the Caribbean, including the southern latitude obtained in this contribution (*Boschman et al., 2014* and *Weber et al., 2015*); paleolongitude is speculative. The star represents the mean direction found in this study at 100 Ma. CLIP: Caribbean Large Igneous Province.

and the geochemical and temporal features of the volcanic rocks exposed at the bottom of the Caribbean Sea and its margins (reviews in *Pindell and Keenan, 2009*).

Whether the origin of this volcanic province is linked to a plume or a plate tectonics dominated scenario is a fundamental question (*Hastie and Kerr, 2010*; *Serrano et al., 2011*). However, the major controversy on the origin of the Caribbean plate has been its paleogeography (*Pindell and Kennan, 2009*). Currently most researchers considered the allochthonous model as plausible, as it appropriately explains the contrast in the geological record between the margin of the Americas and the accreted oceanic fragments that limit the Caribbean oceanic crust (active vs passive margin or shallow vs deep marine conditions), as well as the existence of geophysical evidence of a long Atlantic slab under the Caribbean crust (*Pindell and Kennan, 2009*; *Bezada et al., 2010*; *Boschman et al., 2014*).

Given the lack of sea floor magnetic anomalies to constrain plate tectonic reconstructions, the paleogeography of the Caribbean Plate inevitably remains an open question (*Counil et al., 1989*; *Acton, 2000*). Recent reviews compiling regional geological data that try to fit the different magmatic, sedimentary and metamorphic record on the Circum-Caribbean and Northern Andes, have suggested that the Caribbean plate was formed farther south, but in a western position unrelated to the Galapagos hot spot (*Boschman et al., 2014*).

We have obtained paleomagnetic results on three sites of volcanic and plutonic rocks in the northern segment of the Western Cordillera of Colombia, which based on their compositional characteristics, have been related to the Cretaceous oceanic plateau that experienced the superposition of an intra-oceanic arc setting (*Kerr et al., 1997*; *Rodriguez and Arango, 2012*; *Zapata et al., 2017*). Age constraints for the sampled sites, which might be used for paleolatitudinal analysis include: 1) the 87 Ma crystallization ages of the sampled gabbroic body (Fig. 3b), 2) Berriasian to Albian fossil ages in the interstratified sediments (*Gonzalez, 2001*; *Pardo-Trujillo et al., 2002*; Fig. 3a,c),

and 3) a ca. 100 Ma age from a tonalitic intrusion in the northernmost sites. These three pieces of evidence suggest that the sampled lavas are older than 87 Ma.

Taking into account that the tilt-correction tests do not allow to document the timing of magnetization in relation with deformation, we discuss two possible scenarios for the obtained paleomagnetic directions in the Altamira area: 1) the characteristic magnetization component (*ChRM*) represents a primary magnetization acquired in southern paleolatitudes during the Cretaceous normal superchron (83 to 126 Ma), expecting a northern declination and a negative inclination; or 2), the *ChRM* is related to a secondary magnetization event in northern paleolatitudes in a reverse interval of the Earth's magnetic field in the Cenozoic, expecting a southern declination and negative shallow inclination. As discussed below, we consider that the first scenario agrees with the Pacific origin of the Caribbean plate.

For the first scenario, since primary magnetization must have been acquired during the Cretaceous normal superchrom, negative inclinations found at the sites in Altamira is consistent with magnetization recorded in southern latitudes. An allochtonous origin with later accretion and additional dextral strike-slip deformation could then be responsible for the negative inclinations with southern declinations (tilt-corrected direction $D = 130.3°$, $I = –23.3°$, $k = 23.4$, $\alpha_{95} = 26°$). The calculated paleolatitudinal values varied between 21°S and 4°S, with a mean of 12°S, which is south of Galápagos, and therefore consistent with a southern Pacific position of this block in the Late Cretaceous (Fig. 12).

Other paleomagnetic studies carried out in volcanic rocks of oceanic origin and related to these oceanic accreted terranes have yielded similar conclusions. The formation of the Caribbean plate in paleolatitudes to the south of its present position has been constrained by previous paleomagnetic studies. 1) The Western Cordillera of Ecuador, in the Pallatanga block, that is characterized by an oceanic plateau origin and a Caribbean plate affinity (*Roperch et al., 1987*; *Mourier et al., 1988*; *Luzieux et al., 2006*; *Vallejo et al., 2006*), 2) the southern segment of the Western Cordillera of Colombia, south of our sampled localities (*Estrada, 1995*; *MacDonald et al., 1997*), 3) Panama (*Montes et al., 2012*), 4) the Leeward Antilles (*Stearns et al., 1981*), and 5) in the Colombian basin (*Acton, 2000*). Therefore, the hypothesis of the origin in southern paleolatitudes of basalts and gabbros exposed in the northern segment of the Western Cordillera of Colombia (Fig. 3b) is plausible, although a much larger paleomagnetic database is needed for a conclusive answer.

Once the Caribbean oceanic plateau, including the Colombian basalts, was formed in southern latitudes, a new subduction zone seems to be established at its margins, as suggested by the presence of tonalitic bodies and gabbros (such as the Altamira Gabbro, Buga and Sabanalarga Batholiths) with ages between 87 Ma and 80 Ma (*Ordoñez et al., 2011*; *Pindell and Kennan, 2009*; *Villagómez et al., 2011*; *Wrigth and Wyld, 2011*; *Weber et al., 2015*; *Whattam and Stern, 2014*; *Zapata et al., 2017*; Figs 13 and 14). This block began its approach to the continental margin until it collided by 70–75 Ma, as suggested by the exhumation history of the margin and the major changes in the sedimentary patterns of the eastern basins of Colombia and Ecuador (*Villamil, 1999*; *Vallejo et al., 2006*; *Villagómez et al., 2011*; *Spikings et al., 2016*; *Zapata et al., 2017*). During the accretion, some remnants of the oceanic arc and plateau crust were extensively deformed, forming a greenschist facies mylonitic belt (*Guiral-Vega et al., 2015*).

Although our results are still limited, the paleolatitudinal record found in Caribbean and Northern South American sites (*Stearns et al., 1981*; *Estrada, 1995*; *Acton, 2000*; *Luzieux et al., 2006*; *Montes et al., 2012*; *Boschman et al., 2014*), the size of the thick Caribbean plate and the accreted fragments in the Northern Andes and the Caribbean Antilles is compatible existence of a broad plateau province. The apparent coherence of the high-density block with lack of positive anomalies inferred from the gravimetric results in the northern segment of the Western Cordillera of Colombia also suggest that this fragments may be part of a single plateau unit.

7.3. Block rotation constraints

Paleomagnetic results also document major rotations, either 130° clockwise (scenario 1) or 50° counter-clockwise rotations (scenario 2). In both scenarios, the rotation pattern can be associated with the Romeral strike-slip Fault (Fig. 2), and the counter-clockwise rotations patterns into a predominantly dextral shear can be explained by a discontinuous model (*García and Jiménez, 2016*). According to *Hernandez-Moreno et al. (2014)*, different geometric models have been proposed to explain the pattern of deformation and vertical-axis rotation in strike-slip fault zones. Depending on block size and shape, and the rotation pattern, models can be subdivided into three main groups, called discontinuous, continuous, or quasi-continuous models (*Hernandez-Moreno et al., 2014*).

The rotation pattern in the first scenario means rotations > 90° (Fig. 13). In this scenario, the clockwise rotations (approximately 130°) are related to a complex kinematic setting associated to the accretion and additional dextral strike-slip deformation between oceanic and continental crust. Deformation and vertical axis rotations are related to a quasi-continuos model (Fig. 13a). Similar clockwise block rotations of ca. 90° and northern translation have also been documented in the Western Cordillera of Ecuador (*Luzieux et al., 2006*). *MacDonald et al. (1996)* documented 30° of clockwise rotation in Late Miocene porphyritic intrusions in the Cauca valley within the Romeral fault system, which are located immediately to the east of the sampled localities. Although a precise timing of the suggested block rotation cannot be guaranteed, the more extensive rotation recorded in the sampled Cretaceous rocks is compatible with the existence of pre-Miocene events related to the plateau collision. In the alternative scenario, the counter-clockwise rotations can be related to secondary faults formed in a discontinuous model during the Cenozoic (Fig. 13b).

8. CONCLUSIONS

Gravimetric and preliminary paleomagnetic constraints from the northern segment of the Western Cordillera of Colombia suggest the existence of a coherent high density block of Early to Late Cretaceous that was formed at southern latitudes in the Pacific as part of an oceanic plateau and intra-oceanic arc that was subsequently accreted, dismembered and rotated along the continental margin. This block is part of a broader province that includes the southern segments of the western Colombian and Ecuadorian Andes and formed a major Cretaceous large igneous province that can be related to the Caribbean plate, whose inception between the Americas was responsible for the initiation of the Andean

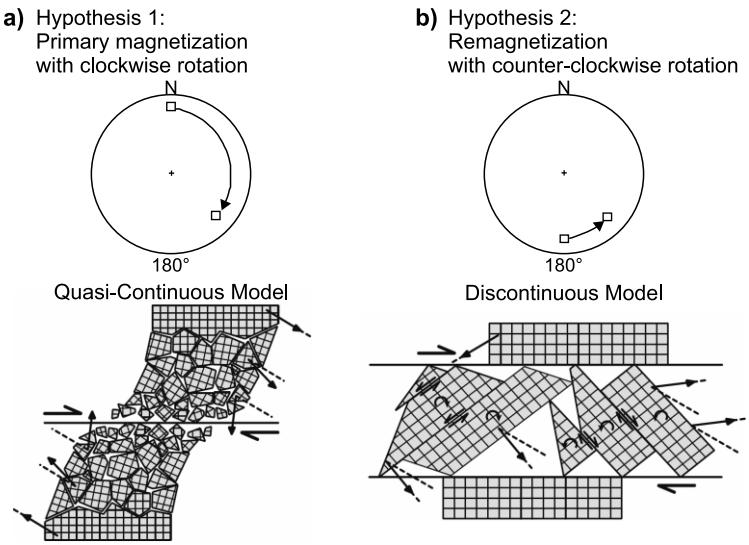

Fig. 13. Kinematic models of strike-slip fault or shear zones and the relationship with the sense and amount of vertical rotations; **a)** quasi-continuous model: small-block model to explain clockwise rotations (> 90°) (scenario 1), and **b)** discontinuous or discrete model: conjugate set of bounding faults into a strike-slip domain to explain counter-clockwise rotations (scenario 2). In both scenarios, rotations are related to the dextral strike slip Romeral Fault system. Arrows represent rotations and dashed lines represent the unrotated magnetization direction. (Redrawn from *Hernandez-Moreno et al., 2014*).

orogeny. Paleomagnetic data acquired in this study suggest that the Cretaceous of the Western Colombian Andes has the potential of being evaluated with paleomagnetic methods. A more detailed and systematic paleomagnetic study in structurally- and age-constrained oceanic volcanic and sedimentary rocks in this region are necessary for a more precise and reliable reconstruction.

Acknowledgements: We acknowledge the magnetic laboratory team from the Instituto de Astronomia, Geofísica é Ciencias Atmosfericas of the University of Sao Paulo (Brazil) for the access to the Paleomagnetic facilities, and the Asociación Colombiana de Geólogos y Geofísicos del Petróleo (ACGGP) for the CORRIGAN-ACGGP-ARES grant to Santiago Hincapié. We kindly acknowledge comments and suggestions of Fernando Poblete and an anonymous reviewer, as well as the editorial efforts of Augusto Rapalini and Avto Goguishaishvilli. The National University of Colombia is greatly acknowledged for its financial support with grant 30362, whereas the 2014 EGEO students are also acknowledge for their help during fieldwork and discussions.

References

Acton G.D., Galbrun B. and King, J.W., 2000. Paleolatitude of the Caribbean plate since the Late Cretaceous. In: Leckie R.M., Sigurdsson H., Acton G.D. and Draper G. (Eds), *Proceedings of the Ocean Drilling Program, Scientific Results*, **165**, 149-173, DOI: 10.2973 /odp.proc.sr.165.001.2000.

ANH, 2008. *Bouguer Total Anomalies Map for Colombia, Scale 1:2 500 000*. Agencia Nacional de Hidrocarburos, Bogota, Colombia.

Alvarez A.J. and Gonzalez H., 1979. *Geología y geoquímica del cuadrángulo I-7. Informe n° 1761*. Ministerio de Minas y Energía, Instituto de Investigación e Información Geocientífica, Minero-Ambiental y Nuclear – INGEOMINAS, Bogota, Colombia (in Spanish).

Bayona G., Rapalini A. and Constanzo-Alvarez V., 2006. Paleomagnetism in Mesozoic rocks of the Northern Andes and its Implications in Mesozoic tectonics of Northwestern South America. *Earth Planets Space*, **58**, 1255–1272.

Bezada M.J., Levander A. and Schamandt B., 2010. Subduction in the southern Caribbean: Images from finite-frequency P wave tomography. *J. Geophys. Res.*, **115**, B12333, DOI: 10.1029/2010JB007682.

Boschman L., Hinsbergen D., Torsvik T., Spakan W. and Pindell J., 2014. Kinematic reconstruction of the Caribbean region since the Early Jurassic. *Earth Sci. Rev.*, **138**, 102–136.

Burger H.R., Sheehan A.F. and Jones C.H., 2006. *Introduction to Applied Geophysics: Exploring the Shalow Subsurface*. W.W. Norton & Company, New Yprk, 554 pp.

Burke K., 1988. Tectonic evolution of the Caribbean: *Ann. Rev. Earth Planet. Sci.*, **16**, 210–230.

Case J.E., Duran L.G., Lopez R.A. and Moore W.R., 1971. Tectonic investigations in Western Colombia and eastern Panama. *Geol. Soc. Am. Bull.*, **82**, 2685–2712.

Case J.E., MacDonald W.D. and Fox P.J., 1990. Caribbean crustal provinces; seismic and gravity evidence. In: Dengo G. and Case J.E. (Eds), *The Caribbean Region*. Geological Society of America, Boulder, CO, 15–36.

Cawood P.A., Kröner A., Collins W.J., Kusky T.M., Mooney W.D. and Windley B.F., 2009. Accretionary orogens through Earth history. *Geol. Soc. London Spec. Publ.*, **318**, 1–36.

Chiarabba C., De Gori P., Faccenna C., Speranza F., Seccia D., Dionicio V. and Prieto G.A., 2016. Subduction system and flat slab beneath the Eastern Cordillera of Colombia. *Geochem. Geophysics Geosystems*, **17**, 16–27.

Christensen N.I. and Mooney W.D., 1995. Seismic velocity structure and composition of the continental crust: A global view. *J. Geophys. Res.*, **100(B7)**, 9761–9788.

Cochrane R., Spikings R., Gerdes A., Winkler W., Uliano A., Mora A. and Chiaradia M., 2014. Distinguishing between in-situ and accretionary growth of continents along active margins. *Lithos*, **202–203**, 382–394.

Counil J.L., Achache J. and Galdeano A., 1989. Long-wavelenght magnetic anomalies in the Caribbean: Plate boundaries and allochtonous continental blocks. *J. Geophys. Res.*, **94**, 7419–7431.

Demarest H., 1983. Error analysis for determination of tectonic rotation from paleomagnetic data. *J. Geophys. Res.*, **88**, 4321–4328.

Diebold J. and Driscoll N., 1999. New Insights on the Formation of the Caribbean Basalt Province revealed by Multichannel seismic images of volcanic structures in the Venezuelan basin. *Sedimentary Basins of the World*, **4**, 561–589.

Duque-Caro H., 1990. The Choco Block in the northwestern corner of South America: Structural, tectonostratigraphic, and paleogeographic implications. *J. South Am. Earth Sci.*, **3**, 71–84.

Estrada J.J., 1995. *Paleomagnetism and Accretion Events in the Northern Andes*. MSc Thesis. State University of New York, Binghamton, NY.

Etayo-Serna F., 1989. Campanian to Maastrichtian fossils in the Northeastern Western Cordillera, Colombia. *Geología Norandina*, **2**, 25–30.

Fisher R.A., 1953. Dispersion on a sphere. *Proc. R. Soc. London A*, **217**, 295–305.

Flueh E.R., Milkereit B., Meissner R., Meyer R.P., Ramirez J.E., Quintero J.C. and Udias A., 1981. Seismic refraction observations in northwestern Colombia at latitude 5.5°N. In: Miller H. and Rosenfeld U. (Eds), *Zentralblatt fuer Geologie and Palaeontologie*, *Teil I, Allgemeine, Angewandte, Regionale and Historische Geologie*, **3–4**, 231–242.

Franco H. and Abbott D., 1999. Gravity signatures of terrane accretion. *Lithos*, **46**, 5–15.

Garcia H. and Jiménez G., 2016. Transverse zones controlling the structural evolution of the Zipaquira Anticline (Eastern Cordillera, Colombia): Regional implications. *J. South Am. Earth Sci.*, **69**, 243–258.

Gonzalez H., 2001. *Mapa geológico del departamento de Antioquia. Memoria explicativa*. Ministerio de Minas y Energía, Instituto de Investigación e Información Geocientífica, Minero-Ambiental y Nuclear - INGEOMINAS, Bogota, Colombia (in Spanish).

Guiral-Vega J.S., Rincon-Gamero J. and Ordoñez-Carmona O., 2015. Geology of the southern part of Sabanalarga Batholith: Implications for terrane theory in the west of Colombia. *Boletin Ciencias de la Tierra*, **38**, 41–48.

Hall R.B. and Alvarez R.H., 1972. *Geología de la parte de los departamentos de Antioquia y Caldas (sub-zona II-A)*. Boletín Geológico, Ministerio de Minas y Energía, Instituto de Investigación e Información Geocientífica, Minero-Ambiental y Nuclear - INGEOMINAS, Bogota, Colombia (in Spanish).

Hastie A.R., Kerr A.C., Mitchell S.F. and Millar I.L., 2008. Geochemistry and petrogenesis of Cretaceous oceanic plateau lavas in eastern Jamaica. *Lithos*, **101**, 323–343.

Hastie A.R. and Kerr A.C., 2010. Mantle plume or slab window? Physical and geochemical constraints on the origin of the Caribbean oceanic plateau. *Earth Sci. Rev.*, **98**, 283–293.

Hernandez-Moreno C., Speranza F. and Di Chiara A., 2014. Understanding kinematics of intra-arc transcurrent deformation: paleomagnetic evidence from the Liquiñe-Ofqui fault zone (Chile, 38°–41°S). *Tectonics*, **33**, 1964–1988.

Hoernle K., van den Bogaard P., Werner R., Lissinna B., Hauff F., Alvarado G. and Garbe-Schönberg D., 2002. Missing history (16–71 Ma) of the Galápagos hotspot: Implications for the tectonic and biological evolution of the Americas. *Geology*, **30**, 795–798.

Jaillard E., Lapierre H., Ordoñez M., Toro J., Amórtegui A. and Vanmelle J., 2009. Accreted oceanic terranes in Ecuador: Southern edge of the Caribbean plate? *Geol. Soc. London Spec. Publ.*, **328**, 469–485.

James K.H., 2006. Arguments for and against the pacific origin of the Caribbean Plate: discussion, finding for an inter-American origin. *Geologica Acta*, **4**, 1–2, 279–302.

James K.H., 2009. In situ origin of the Caribbean: discussion of data. *Geol. Soc. London Spec. Publ.*, **328**, 77–125.

Kerr A.C., Marriner G.F., Tarney J., Nivia A., Saunders A.D, Thirwall M.F. and Sinton C.W., 1997. Cretaceous Basaltic Terranes in Western Colombia: Elemental, chronological and Sr-Nd isotopic constraints on petrogenesis. *J. Petrol.*, **38**, 677–702.

Kerr A.C., Tarney J., Kempton P.D., Spadea P., Nivia A., Marriner G.F. and Duncan R.A., 2002. Pervasive mantle plume head heterogeneity: Evidence from the late Cretaceous Caribbean-Colombian oceanic plateau. *J. Geophys. Res.*, **107**, 2140, DOI: 10.1029/2001JB000790.

Kirschvink J., 1980. The least-squares line and plane and the analysis of paleomagnetic data. *Geophys. J. R. Astron. Soc.*, **62**, 699–718.

Lowrie W., 1990. Identification of ferromagnetic minerals in a rock by coercivity and unblocking temperature properties. *Geophys. Res. Lett.*, **17**, 159–162.

Luzieux L.D.A., Heller F., Spikings R., Vallejo C.F. and Winkler W., 2006. Origin and Cretaceous tectonic history of the coastal Ecuadorian forearc between 1°N and 3°S: Paleomagnetic, radiometric and fossil evidence. *Earth Planet. Sci. Lett.*, **249**, 400–414.

MacDonald W.D., Estrada J.J., Sierra G.M. and Gonzalez H., 1996. Late Cenozoic tectonics and paleomagnetism of North Cauca Basin intrusions, Colombian Andes: Dual rotation modes. *Tectonophysics*, **261**, 277–289.

MacDonald W.D., Estrada J.J. and Gonzalez H., 1997. Paleoplate affiliations of volcanic accretionary terranes of the Northern Andes. *Geological Society of American Abstracts with Programs*, **29**, 245.

Manalo P.C., Dimalanta C.B., Faustino-Eslava D.V., Ramos N.T., Queaño K.L. and Yumul Jr. G.P., 2015. Crustal thickness variation from a continental to an island arc terrane: Clues from the gravity signatures of the Central Philippines. *J. Asian Earth Sci.*, **104**, 205–214

Mauffret A. and Leroy S., 1997. Seismic stratigraphy and structure of the Caribbean igneous province. *Tectonophysics*, **283**, 61–104.

Maya M. and Gonzalez H., 1995. Unidades litodemicas en la Cordillera Central de los Andes colombianos. *Boletín Geológico INGEOMINAS*, **35**, 43–57.

Montes C., Bayona G., Cardona A., Buchs D.M., Silva C.A., Moron S., Hoyos N., Ramirez D.A., Jaramillo C.A. and Valencia V., 2012. Arc-continent collision and orocline formation: Closing of the Central American seaway. *J. Geophys. Res.*, **117**, B04105, DOI: 10.1029 /2011JB008959.

Montes C., Cardona A., Jaramillo C., Pardo A., Silva J.C., Valencia V., Ayala C., Pérez-Angel L.C., Rodriguez-Parra L.A., Ramirez V. and Niño H., 2015. Middle Miocene closure of the Central American Seaway. *Science*, **348**, 226–228.

Mourier T., Laj C., Mégard F., Roperch P., Mitouard P. and Farfan-Medrano A., 1988. Accreted continental terrane in northwestern Peru. *Earth Planet. Sci. Lett.*, **88**, 182–192.

Nivia A., 1996. The Bolivar mafic-ultramafic complex, SW Colombia: the base of an obducted oceanic plateau. *J. South Am. Earth Sci.*, **9**, 59–68.

Nivia A., 2001. *Mapa geológico del departamento del Valle del Cauca*. Memoria Explicativa. Ministerio de Minas y Energía, Instituto de Investigación e Información Geocientífica, Minero-Ambiental y Nuclear – INGEOMINAS, Bogota, Colombia (in Spanish).

Nivia A., Marriner G.F., Kerr A.C. and Tarney J., 2006. The Quebradagrande Complex: A Lower Cretaceous ensialic marginal basin in the Central Cordillera of Colombian Andes. *J. South Am. Earth Sci.*, **21**, 423–436.

Pardo-Trujillo A., Moreno-Sanchez M. and Gomez-Cruz A., 2002. Stratigraphy of some Upper Cretaceous deposits of the Central and Western Cordilleras of Colombia: regional implications. *Int. J. Trop. Geol. Geogr. Ecol.*, Special Issue **26-2**.

Pindell J.L. and Barret S.F., 1990. Geological evolution of the Caribbean region; A plate-tectonic perspective. In: Dengo G. and Case J.E. (Eds), *The Caribbean Region*. Geological Society of America, Boulder, CO, 405–432.

Pindell J.L. and Kennan L., 2009. Tectonic evolution of the Gulf of Mexico, Caribbean and northern South America in the mantle reference frame: an update. *Geol. Soc. London Spec. Publ.*, **328**, 1–55.

Poveda E., Monsalve G. and Vargas C.A., 2015. Receiver functions and crustal structure of the northwestern Andean Region, Colombia. *J. Geophys. Res.*, **120**, 2408–2425, DOI: 10.1002 /2014JB011304.

Restrepo J.J. and Toussaint J., 1988. Terranes and continental accretion in the Colombian Andes. *Episodes*, **11**, 189–193.

Restrepo J.J, Ordoñez-Carmona O., Martens U. and Correa A.M., 2009. Terrenos, complejos y provincias en la Cordillera Central de Colombia. *I^2+D*, **9**, 49–56 (in Spanish).

Rodríguez G. and Arango M.I., 2013. Formación Barroso: Arco volcánico toleítico y diabasas de San José de Urama: Prisma T-MORB en el segmento norte de la Cordillera Occidental de Colombia. *Boletín Ciencias de la Tierra*, **33**, 17–38 (in Spanish).

Roperch P., Mégard F., Laj C., Mourier T., Clube T.M. and Noblet C., 1987. Rotated oceanic blocks in Western Ecuador. *Geophys. Res. Lett.*, **14**, 558–561.

Safonova I., Utsunomiya A., Kojima S., Nakae S., Tomurtogoo O., Filippov A.N. and Koizumi K., 2009. Pacific superplume-related oceanic basalts hosted by accretionary complexes of Central Asia, Russian Far East and Japan. *Gondwana Res.*, **16**, 587–608.

Sarmiento-Rojas L.F, Van Wess J.D. and Cloetingh S., 2006. Mesozoic transtensional basin history of the Eastern Cordillera, Colombia Andes: Inferences from tectonic models. *J. South Am. Earth Sci.*, **21**, 383–411.

Serrano L., Ferrari L., Lopez M., Petrone C.M. and Jaramillo C., 2011. An integrative geologic, geochronologic and geochemical study of Gorgona Island, Colombia: Implications for the Caribbean Large Igneous Province. *Earth Planet. Sci. Lett.*, **309**, 324–336.

Sinton C.W., 1998. An oceanic flood basalt province within the Caribbean Plate. *Earth Planet. Sci. Lett.*, **155**, 221–235.

Spikings R., Cochrane R., Villagómez D., Van der Lelij R., Vallejo C., Winkler W. and Beate B., 2015. The geological history of northwestern South America: From Pangea to the early collision of the Caribbean Large Igneous Province (290-75 Ma). *Gondwana Res.*, **27**, 95–139.

Spikings R., Reitsma M.J., Boekhout F., Miskovic A., Ulianov A., Chiaradia M., Gerdes A. and Schaltegger U., 2016. Characterization of Triassic rifting in Peru and implications for the early disassembly of western Pangea. *Gondwana Res.*, **35**, 124–143.

Stearns C., Mauk F.J. and Van der Voo R., 1981. Late Cretaceous-Early Tertiary paleomagnetism of Aruba and Bonaire (Netherlands Leeward Antilles). *J. Geophys. Res.*, **87**, 1127–1141.

Syracuse E.M., Maceira M., Prieto G.A., Zhang H. and Ammon C.J., 2016. Multiple plates subducting beneath Colombia, as illuminated by seismicity and velocity from the joint inversion of seismic and gravity data. *Earth Planet. Sci. Lett.*, **444**, 139–149.

Torsvik T.H., Müller R., Van der Voo R., Steinberger B. and Gaina C., 2008. Global plate motion frames: Toward a unified model. *Rev. Geophys.*, **46**, RG3004, DOI: 10.1029/2007RG000227.

Torsvik T.H., Van der Voo R., Preeeden U., Niocaill C., Steinberger B., Doubrovine P.V., Van Hinsbergen D.J., Domeier M., Gaina C., Meert J.G., McCausland P.J. and Cocks L.R., 2012. Phanerozoic polar wander, paleogeography and dynamics. *Earth Sci. Rev.*, **114**, 325–368.

Vallejo C., Spikings R., Luzieux L., Chew D. and Page L., 2006. The early interaction between the Caribbean Plateau and the NW South American Plate. *Terra Nova*, **18**, 264–269.

Van der Lelij R., Spikings R., Kerr A.C., Kounov A., Cosca M., Chew D. and Villagómez D., 2010. Thermochronology and tectonics of the Leward Antilles: Evolution of southern Caribbean Plate boundary zone. *Tectonics*, **29**, TC6003, DOI: 10.1029/2009TC002654.

Villagómez D., Spikings R., Magna T., Kammer A., Winkler W. and Beltrán A., 2011. Geochronology, geochemestry and tectonic evolution of the Western and Central cordilleras of Colombia. *Lithos*, **125**, 875–896.

Villamil T., 1999. Campanian-Miocene tectonostratigraphy, depocenter evolution and basin development of Colombia and Western Venezuela. *Paleogeogr., Paleoclimatol. Paleoecol.*, **153**, 239–275.

Villarraga C., Lopez M. and Cardona A., 2016. *Temporalidad y características geoquímicas del vulcanismo cretácico del sector norte de la Cordillera Occidental colombiana: Implicaciones tectónicas*. MSc Thesis. Centro de Investigación Científica y de educación Superior de Ensenada, Baja California, CICESE, Ensenada, Mexico (in Spanish).

Vinasco C.J., Cordani U.G., Gonzalez H., Weber M. and Pelaez C., 2006. Geochronological, isotopic, and geochemical data from Permo-Triassic granitic gneisses and granitoids of the Colombian Central Andes. *J. South Am. Earth Sci.*, **21**, 355–371.

Weber M., Gomez-Tapias J., Cardona A., Duarte E., Pardo-Trujillo A. and Valencia V., 2015. Geochemistry of the Santa Fé Batholith and Buriticá Tonalite in NW Colombia - Evidence of subduction initiation beneath the Colombian Caribbean Plateau. *J. South Am. Earth Sci.*, **62**, 257–274.

Whattan S.C. and Stern R.J., 2014. Late Cretaceous plume-induced subduction initiation along the southern margin of the Caribbean and NW South America: The first documented example with implications for the onset of Plate Tectonics. *Gondwana Res.*, **27**, 38–63.

Wright J.E. and Wyld S.J., 2011. Late Cretaceous subduction initiation on the eastern margin of the Caribbean-Colombian Oceanic Plateau: one great arc of the Caribbean (?). *Geosphere*, **7**, 468–493.

Yarce J., Monsalve G., Becker T.W., Cardona A., Poveda E., Alvira D. and Ordoñez-Carmona O., 2014. Seismological observations in Northwestern South America: Evidence for two subduction segments, contrasting crustal thicknesses and upper mantle flow. *Tectonophysics*, **637**, 57–67.

Zapata J.P., Restrepo J.J., Cardona A. and Martens U., 2017. Geoquímica y geocronología de las rocas volcánicas básicas y el gabro de Altamira, Cordillera Occidental (Colombia): Registros de ambientes de Plateau y Arco oceánico superpuestos durante el cretácico. *Boletín de Geología*, **39**, 13–30, DOI: 10.18273/revbol.v39n2-2017001 (in Spanish).

Zijderveld J.D., 1967. A.C. demagnetization of rocks: analysis of results. In: Collison D.W., Creer K.M. and Runcorn S.K. (Eds), *Methods of Paleomagnetism*. Elsevier Science, Amsterdam, The Netherlands, 254–286.